# Binding energy and structure of the ground, first electronic and ion states of p-methoxyphenethylamine(H2O)1 isomers: A combined experimental and theoretical study

**ARTICLE** *in* CHEMICAL PHYSICS · SEPTEMBER 2001

Impact Factor: 1.65 · DOI: 10.1016/S0301-0104(01)00421-9



**5 AUTHORS**, INCLUDING:

José Andrés Fernández
Universidad del País Vasco / Euskal He…

**118** PUBLICATIONS **869** CITATIONS

SEE PROFILE

ELSEVIER

Chemical Physics 271 (2001) 55–69

Chemical Physics

www.elsevier.com/locate/chemphys

# Binding energy and structure of the ground, first electronic and ion states of *p*-methoxyphenethylamine$(H_2O)_1$ isomers: a combined experimental and theoretical study

Iñigo Unamuno, José A. Fernández, Carlos Landajo, Asier Longarte, Fernando Castaño *

*Departamento de Química-Fisica, Facultad de Ciencias, Universidad del País Vasco, Apartado 644, 48080 Bilbao, Spain*

Received 9 April 2001

**Abstract**

An extensive laser spectroscopic, structural and computational investigation on the neurotransmitter analogue *p*-methoxyphenethylamine (MPEA) chromophore weakly bound to one molecule of water, (MPEA$(H_2O)_1$) is reported. The complex was prepared by supersonic expansion of a gas mixture of seeded MPEA and water molecules in rare gas He. Two well-characterised experimental isomers have been observed, with geometries resulting from large contributions of the ordinary hydrogen bond and other intermolecular forces. Four key properties of the complex and related species are addressed in this paper: the characterisation of the isolated isomers observed spectra, the measurements of the binding energies of the ground, first electronic and ground ion states of the complex, the identification of each isomer spectrum with the computed geometries and the relationship of the complex stable isomers with the precursor conformers. A number of mass resolved laser spectroscopies have been used in order to get a complete set of experimental results, that complemented with ab initio density functional computations at four basis set, finally permitted us to settle and assign the mentioned properties of the two observed MPEA$(H_2O)_1$ isomers. 

## 1. Introduction

The *p*-methoxyphenethylamine (MPEA) molecule is an analogue to tyramine, a well-known neurotransmitter molecule [1]. Other members of the family include phenethylamine (PEA), adrenaline and mescaline (Fig. 1) [2–6]. These molecules have in common one ethylamino group bonded to a benzene ring, two functional groups that seem to be the fundament of their biological activity. The flexibility of the ethylamino chain gives rise to a number of conformers, generated by rotation around the $C_\alpha$–$C_\beta$ and $C_\alpha$–$NH_2$ bonds in the standard nomenclature (cf. Fig. 1). The rotation around the $C_\alpha$–$C_\beta$ bond originates two sets of conformers' known as *anti* or extended and *gauche* or folded, whose difference is the presence of an $NH_2$-aromatic ring intramolecular interaction in the *gauche* conformer. The stability of both sets of conformers is similar, since the extra intramolecular interaction in the *gauche* conformers is in

* Corresponding author. Tel.: +34-94-601-2533; fax: +34-94-464-8500.

*E-mail address:* qfpcaalf@lg.ehu.es (F. Castaño).

0301-0104/01/$ - see front matter 
PII: S0301-0104(01)00421-9

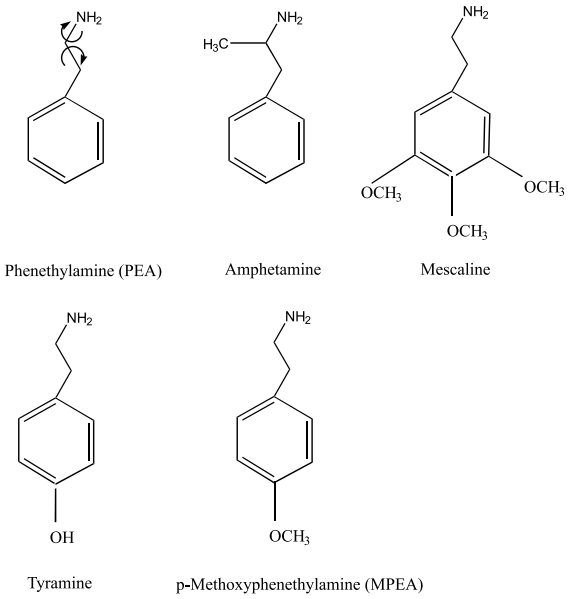


Fig. 1. Some significant molecules of the tyramine family of neurotransmitters.

part compensated by the unfavourable interaction between the $C_\alpha H_2$ and $C_\beta H_2$ groups H atoms, which are partially eclipsed. The rotation of the $NH_2$ group has almost no effect on the stability of the *anti* conformers, because this group is far from the aromatic ring. In contrast, the *gauche* conformers have an $NH_2 \cdots \pi$ interaction in addition to that of the N atom lone pair and the aromatic ring, resulting in a larger energy difference and stability between the *gauche* conformers.

The rotation around the $C_\alpha$–$C_\beta$ and $C_\alpha$–$NH_2$ bonds in the phenethylamine, the simplest molecule of the neurotransmitter family, leads to five experimentally distinguishable conformers [4]. *Para*-substitution of the aromatic ring by OH or O–$CH_3$ groups induces an asymmetry in the chromophore, increasing the number of conformers (Fig. 1) – from the five PEA conformers to the nine of MPEA [7]. In consequence, the energy of the conformers turns out to be very close and the spectral bands overlapped, powerful spectroscopic techniques being required to distinguish their properties. Mass-resolved excitation spectroscopy (MRES), carried out with one-colour (REMPI) or two-colour (R2PI) lasers, mass-resolved IR–UV double resonance and "hole burning" (HB) spectroscopies, combined with supersonic expansions to freeze down rotations and vibrations to finally yield ground state complexes, are required for the study. In addition, the isolated species characteristic of the pulsed expansion allows a direct comparison between the experimental spectra and the ab initio calculated properties. In recent studies, the application of the aforementioned techniques resulted in the assignment of the gas-phase spectra of PEA [4,5] and MPEA [1] molecules. Further comparison with ab initio calculations, has led to the structural identification of their most stable conformers and also their vibrations [7].

However, the biological activity of these molecules takes place in solution. In the presence of water, the relative stability of the folded *gauche* conformers may change considerably; the water molecule attached to the amino group may also interact with the aromatic ring, increasing the energy difference between *anti* and *gauche* conformers. Structural characteristics of this type may unravel the mechanism by which neurotransmitters play their biological role. The link between the properties in solution and the complex created by supersonic expansion relies on the analysis and extrapolation of the properties of the complexes with one to many solvent molecules. However, the addition of one solvent to the chromophore very often produces the largest changes in structure and stability, whereas addition of further solvents only has minor influences. In this paper, we report the spectroscopic changes of MPEA chromophore attached to one water molecule. In fact, the formation of the $MPEA(H_2O)_1$ complex, also referred to later as 1:1 complex, changes the relative stability of the MPEA bare molecule species, decreasing the number of conformers from seven to only two in the 1:1 complex. Furthermore, the comparison with the calculations conducted at the B3LYP method with a number of basis sets – namely 6-31g, 6-31+g(d), 6-311+g(d), AUG-cc-pVDZ – permits the identification of the experimental spectral bands of the isomers to computed stable structures and fine tuning the calculation level required to describe both the complex geometry and the binding energy.

## 2. Method and experimental set-up

The method used to evaluate the binding energies is based on the determination of the ionisation energies (IEs) of both the bare conformers and the isomers, and is referred to as the threshold fragmentation method [8,9]. Fig. 2 outlines the one-dimensional PES of the ground, first electronic excited and the ion ground states, as well as the correlated dissociation solute, M, $M^*$ and $M^+$ and the solvent, S, states. The dissociation energies of the three states considered are related to the following measured IEs (see Fig. 2 for nomenclature):

$$D_0(I_0) = MS(\text{fragment}) - M(I_0 \leftarrow S_1) \quad (1)$$

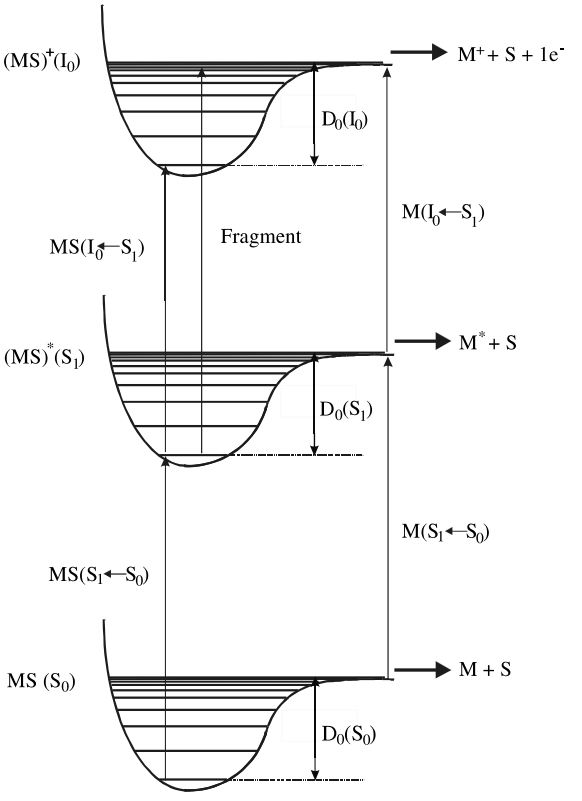


Fig. 2. Schematic representation of the one-dimensional potential energy for the ground, first electronic excited states and ion ground state of a weakly bound isomer, MS. Dissociation or binding energies are indicated by $D_0$ followed by the state considered and transitions such as MS (final ← initial state) and M (final ← initial state) respectively.

$$D_0(S_0) = MS(\text{fragment}) + MS(S_1 \leftarrow S_0) - M(I_0 \leftarrow S_1) - M(S_1 \leftarrow S_0) \quad (2)$$

$$D_0(S_1) = D_0(S_0) + M(S_1 \leftarrow S_0) - MS(S_1 \leftarrow S_0) \quad (3)$$

where $M(S_1 \leftarrow S_0) - MS(S_1 \leftarrow S_0)$ is the complex origin band shift with respect to that of the bare molecule $0_0^0$ transition and "fragment" stands for the energy necessary to ionise the $MS^*$ species and to simultaneously evaporate one solvent molecule. According to Eqs. (1)–(3) a knowledge of the solvents and the complex, (MS), $S_1 \leftarrow S_0$ transition energies, the ionisation and the fragmentation energy thresholds of $MS^+$ to $M^+$ and S, allows one to determine the ground $MS(S_0)$, first electronic $MS(S_1)$ and ion $MS(I_0)$ binding energies. The application of the method has some difficulties and drawbacks: first, if the $I_0 \leftarrow S_1$ transition is associated with a large geometry change, the ionisation threshold is not well defined because of the uncertainties introduced by the characteristic slow slope. In addition, the chromophore intramolecular and the complex intermolecular vibrations must be strongly coupled in order to get a fast energy transfer to the vibrations that drive the system to dissociation. If these conditions are fulfilled, the complex' three states binding energies can be determined to a satisfactory accuracy.

The experimental set-up used has been reported elsewhere [10], and only a brief description is offered here. A mixture of seeded MPEA and water in He, is expanded through a pulsed electromagnetic valve into an evacuated R.M. Jordan time of flight (TOF) chamber. The gas mixture has a typical backing pressure of 3 bar and the vacuum chamber is maintained at $6 \times 10^{-8}$ bar. In the adiabatic expansion, the water and MPEA degrees of freedom are cooled down to a few K, giving rise to the formation of their weak complexes. The pulsed beam is collimated with the aid of a 0.8 mm bore skimmer and enters the TOF ionisation region, where the species are probed with one or two tuneable lasers (depending on the experiment), set in a counterpropagating configuration. The molecules are ionised by multiphoton absorption and detected with a multichannel plate detector

(MCP). The detector signal is routed to a 500 MHz digital oscilloscope (Tektronics TDL 520), where the masses are identified and the signal integrated. The resulting data are sent to a PC-computer for storage and further analysis.

Two tuneable laser systems have been used, one Nd–YAG/dye/SHG (Quantel TDL 90/Quantel YG 980) and one Excimer XeCl/dye/doubling unit (Lambda Physik CompEx 201/Lambda Physic LPD 3000). Laser tuning was accomplished with the aid of either Rhodamine 590, LDS 759, 722 or DCM (Exciton) and monitored in real time by a Fizeau wavelength meter (New Focus model 7711). MPEA was purchased from Sigma-Aldrich Chemicals and used as received; its appropriate vapour pressure and concentration to seed the He mixture was attained by heating the sample at 120°C and keeping the valve at 70°C.

The range of conformers and isomers calculations were carried out with the GAUSSIAN 98W program suite [11] on a number of Intel Pentium III based PC, furnished with 512 Mbytes of RAM memory and 10–20 Gbytes of hard drive.

## 3. Experimental results

In a previous paper [7], the mass-resolved spectroscopy of the bare MPEA chromophore was comprehensively discussed. The MPEA molecule spectrum overlaps with that of the $MPEA(H_2O)_1$ complex, that in addition exhibits some fragmentation, being advisable the use of two-colour spectroscopies to separate the spectra by their masses. Fig. 3 shows the MPEA R2PI spectrum in the 35,500–35,800 $cm^{-1}$ region, scanned by setting the ionisation laser at 29,600 $cm^{-1}$. Seven band origins, labelled by capitals $A, B, \ldots, G$ were identified by Levy and coworkers, [1] as associated

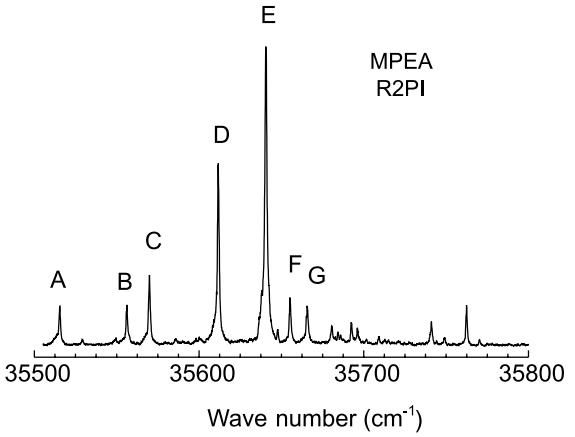


Fig. 3. Two-colour R2PI spectrum of MPEA in a supersonic expansion in buffer He in the 35,500–35,800 $cm^{-1}$ region. The origin band of the seven conformers – four *gauche* and three *anti* – are labelled as $A, B, \ldots, G$.

to the same number of conformers. In the mentioned paper and in a more recent work [7], the conformers were identified and assigned to calculated geometries as follows: bands A–D to *gauche* conformers and bands E, F and G to *anti* conformers (see below). Furthermore, their IEs were measured and are presented in Table 1, together with the seven origin bands wave numbers. These data will be used below to compute the complex binding energy.

The $MPEA(H_2O)_1$ complex has been observed to fragment by $1 + 1$ multiphoton absorption. For higher solvent complexes (1:$n$, $n > 1$) fragmentation is detected in the 1:1 mass-channel, and thus, the $1 + 1'$ multiphoton absorption is preferred to yield neat spectra. As an example, Fig. 4 shows the $MPEA(H_2O)_1$ R2PI spectrum in the 35,650–35,750 $cm^{-1}$ region, obtained by tuning the ionisation laser at 28,600 $cm^{-1}$. Two significant intense bands are observed at 35,676 and 35,689 $cm^{-1}$. The HB

Table 1
$S_1 \leftarrow S_0$, $I_0 \leftarrow S_1$ transitions and IE in wave numbers for the set of seven MPEA conformers (Ref. [7])

| | Origin | | | | | | |
|---|---|---|---|---|---|---|---|
| | A | B | C | D | E | F | G |
| $S_1 \leftarrow S_0$ | 35,505 | 35,546 | 35,559 | 35,601 | 35,630 | 35,645 | 35,655 |
| $I_0 \leftarrow S_1$ | 28,493 | 28,166 | 28,468 | 28,248 | 28,148 | 28,091 | 28,125 |
| IE | 63,998 | 63,712 | 64,027 | 63,849 | 63,778 | 63,736 | 63,780 |

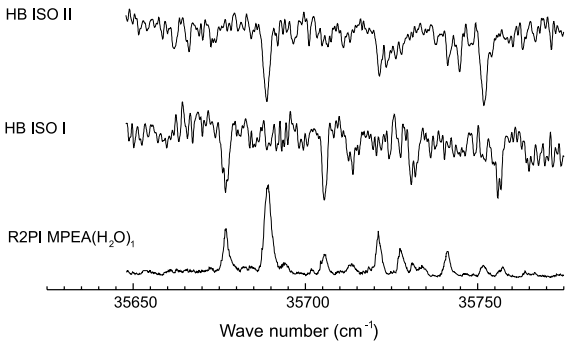


Fig. 4. HB spectra of the $MPEA(H_2O)_1$ isomers I and II, labelled as HB ISO I and HB ISO II respectively. The lower trace is the R2PI $MPEA(H_2O)_1$ spectrum and has been drawn for comparative purposes.

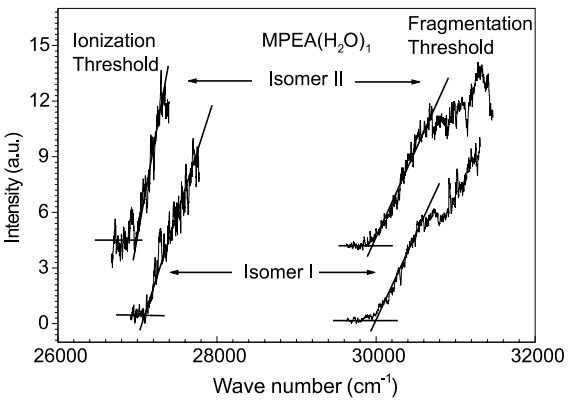


Fig. 5. Example of the ionisation and fragmentation traces and thresholds of the two isomers of the $MPEA(H_2O)_1$ complex. The respective FE and IE values are obtained by adding the $S_1 \leftarrow S_0$ transition energies to the energy threshold values obtained by extrapolation at zero intensity.

spectra recorded by setting the probe laser on these bands, and shown in the upper part of the spectrum for easy comparison, clearly reveal that the two bands correspond to two different isomers of the $MPEA(H_2O)_1$ complex, labelled hereafter as isomers I and II. The HB spectra are noisier than those of R2PI, since they are obtained by $1+1$ multiphoton absorption and therefore, include fragmentation, but the overall signal-to-noise ratio is good enough to identify each band origin with a set of vibrations in the R2PI spectrum.

The experimental profiles to find out the IE and the fragmentation energy (FE) thresholds of the $MPEA(H_2O)_1$ isomers are depicted in Fig. 5. IE profiles were obtained by tuning the probe laser on the selected isomer origin band, scanning the ionisation laser, and detecting at the $MPEA(H_2O)_1$ mass-channel, whilst for FE profiles the detection is at the bare molecule mass-channel. As observed in Fig. 5, both isomers have slightly different IE and FE profiles. Indeed, isomer I has an IE of $(27{,}622 + 35{,}676) = 63{,}298$ $cm^{-1}$ and an FE of $(29{,}808 + 35{,}676) = 65{,}484$ $cm^{-1}$, while the values for the isomer II are: $IE = (27{,}580 + 35{,}689) = 63{,}269$ $cm^{-1}$ and $FE = (29{,}877 + 35{,}689) = 65{,}566$ $cm^{-1}$.

To compute the binding energy of the 1:1 complex, the precursor conformer of each isomer must be known. Applying Eqs. (1)–(3), assuming that any conformer may be the "precursor" of the $MPEA(H_2O)_1$ isomer, the dissociation energies collected in Table 2 are obtained.

## 4. Ab initio calculations

Two goals are sought with the ab initio calculations: to compute the complex binding energy and geometries and to obtain the theoretical data to assign the experimental conformers. The ab initio calculations of $MPEA(H_2O)_1$, have the following challenges: first, it is considered to be a medium-size system by today's computational standards (MPEA has 82 electrons and $MPEA(H_2O)_1$ 92); second, it is a floppy system due to the shallow PES of the weak intermolecular forces involved in the ethylamino chain, and third, there are a number of stable conformers with very close binding energies. Therefore, the optimisations have to be conducted under strict convergence criteria and the BSSE corrections must be kept as low as possible in order to safely choose the most stable conformers. Both aims require the use of large basis sets with polarisation and diffuse functions. In consequence, the theory level and basis set must be carefully chosen, as a compromise between an accurate enough description of the system and a reasonable CPU time. It has been demonstrated [12–16] that some of the recently developed functionals offer a good description of systems with hydrogen bonds (H-bonds), at affordable CPU times. Therefore, we have used Becke's three parameter hybrid functional plus the LYP correlation

Table 2
Computed dissociation energy, $D_0$, for the two MPEA$(H_2O)_1$ isomers, as derived from the set of precursor geometries (A, B, ..., G), and experimental dissociation energy computed with Eqs. (1)–(3), the data listed in Table 1 and the values obtained for the isomers IE and FE[a]

| | Conformer | | | | | | |
|---|---|---|---|---|---|---|---|
| | A | B | C | D | E | F | G |
| *Origin band at 35,676 cm$^{-1}$ (isomer I)* | | | | | | | |
| $D_0(S_0)$ | 1579 | 1865 | 1550 | 1728 | 1799 | 1841 | 1797 |
| Shift[b] | 171 | 130 | 117 | 75 | 46 | 31 | 21 |
| $D_0(S_1)$ | 1408 | 1735 | 1433 | 1653 | 1753 | 1810 | 1776 |
| $D_0(I_0)$ | 2279 | | | | | | |
| *Origin band at 35,689 cm$^{-1}$ (isomer II)* | | | | | | | |
| $D_0(S_0)$ | 1730 | 2016 | 1701 | 1879 | 1950 | 1992 | 1948 |
| Shift[b] | 193 | 152 | 139 | 97 | 68 | 53 | 43 |
| $D_0(S_1)$ | 1546 | 1873 | 1571 | 1791 | 1891 | 1948 | 1914 |
| $D_0(I_0)$ | 2459 | | | | | | |

[a] According to the MPEA conformer chosen, the ground and electronic excited states binding energies, $D_0(S_0)$ and $D_0(S_1)$, vary slightly, but the binding energy of the ion, $D_0(I_0)$, is unaffected.
[b] MPEA$(H_2O)_1$ origin band with shift respect to the MPEA conformers $0_0^0$ transition.

functional, abbreviated as B3LYP, which has been successfully applied to the calculation of similar systems [17–22]. In the present paper calculations with four basis sets have been carried out, namely Pople's 6-31g, 6-31+g* and 6-311+g* and Dunning's correlation consistent AUG-cc-pVDZ. Fig. 6 collects the geometries of the resulting seven most stable MPEA conformers, and Table 3 shows the structural parameter with the largest changes between conformers as computed at the B3LYP/AUG-cc-pVDZ level. Conformers 6 and 9 were not calculated at this level, since they are not detected experimentally probably due to their low stability, whereas they have been considered as possible precursors of the MPEA$(H_2O)_1$ isomers. In Table 3 the proton of the $NH_2$ group interacting with the aromatic ring in the *gauche* conformer has been labelled as $H_a$, while $H_b$ is the proton away from the ring. The same nomenclature will be followed henceforth for the water protons, the shared water proton being referred to as $H_a$ and the unshared one as $H_b$.

Inspection of Table 3 shows that, despite the small energy differences, the conformers stability sequence follows the same pattern for the four basis sets used; hence, any of the three studied basis sets can be successfully applied to describe the bare molecule conformers. In the following we shall refer to the bare molecule conformers as CF$n$, where $n = 1, 2, \ldots, 9$ stand for the conformers number depicted in Fig. 6.

MPEA has five feasible solvation sites: the proton acceptor N atom of the $NH_2$ group, the two proton donor H atoms of the $NH_2$ group, the proton acceptor oxygen lone pairs of the O–$CH_3$ group, and finally the $\pi$ electron cloud. However, according to previous studies [10] the last solvation site is likely to be the less stable and thus it may be neglected. Owing to the bare molecule asymmetry induced by the methoxy group, the two H atoms of the amino group are not equivalent, yielding two different solvation sites, even in the *anti* conformers. In addition to the bare molecule labelling, the isomers are referred to as CF$n$I$m$, where CF$n$ stands for the bare conformer $n$, and $m$ for the arbitrary position in which the water solvent is attached, namely: $m = 1$ for the water bonded to the N–$H_a$, $m = 2$ to the N–$H_b$, $m = 3$ to the N atom and $m = 4$ to the O–$CH_3$ group. Thus, CF4I3 is a complex derived from the conformer 4 and with the water molecule attached to the N atom as a proton donor.

As each conformer is assumed to have four solvation sites and each molecule nine conformers, the expected number of MPEA–water PES minima adds up to 36, a few of them drawn in Fig. 7. Furthermore, there are other possibilities, like the water weakly bonded to the hydrophobic region of

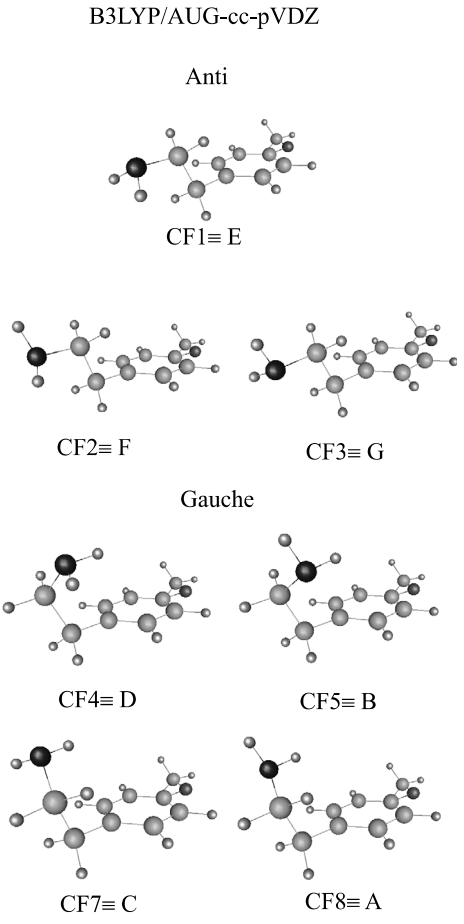


Fig. 6. Stable geometries of the seven conformers of the MPEA, calculated at the B3LYP/AUG-cc-pVDZ level and labelled as CF$n$ ($n = 1$–8) conformer. The assigned band origins are shown in Fig. 3. *Anti* and *gauche* conformers are also labelled.

the MPEA, between the $C_\beta$ and the aromatic ring, opposite to the $NH_2$ group, but all of them have been found to be less stable. In addition, slight changes in the water position leads to relative minima. For instance, the water molecule attached to the $O(CH_3)$ group, with the non-shared proton pointing upwards – with the non-shared proton on the same side of the aromatic ring as the ethylamino group – or downwards, have a conformation energy difference of a mere 14 $cm^{-1}$ ($MPEA(H_2O)_1$ based on CF4, conformer at B3LYP/6-31G level). Alternatively, the rotation around the H-bond of the proton-donor water bonded to the $NH_2$ group (isomer CF1I3 in Fig. 7) computed at the B3LYP/6-31G level yields an energy difference of only 249 $cm^{-1}$.

In Table 4 the binding energies of the isomers calculated at the B3LYP/6-31G level, along with the estimated BSSE, are presented. It is worth noting that of the 36 structures considered, a few of them are unstable, owing to the low potential energy barrier paths to more stable structures. So, CF2I1 and CF2I2 geometries always end in the more stable CF2I3 structure. In almost all the cases, the optimisation of the *gauche*-based isomers with the water bonded to the N–$H_b$ hydrogen, ends up in a structure with the water attached to the N atom, following a long path. More surprising is the optimisation of the isomers based on CF6 and CF9, the less stable bare molecule conformers. Because of the negative interaction between the N lone pair and the aromatic ring $\pi$ electron density, whenever one water molecule is placed close to the $NH_2$ moiety, a rotation around the $C_\alpha$–N bond is induced and the optimisation ends in the CF5I3 and CF8I3 structures, precisely the most stable structures at the present calculation level. From Table 4 it is also evident that at the B3LYP/6-31G calculation level the preferred solvation site is the N atom of the $NH_2$ group (I3 structures), with a binding energy of 2000–3000 $cm^{-1}$ depending on the conformer chosen. However, the large BSSE correction, which is in fact larger than the calculated binding energies difference, precludes a safe identification of the most stable isomer. Therefore, it is advisable to enlarge further the basis sets used so far to obtain sound quantitative conclusions. As I3 was stated to be the set of most stable structures, only these will be examined in the following calculations.

The binding energies of the CF$n$I3 set of structures, with $n = 1$–5, 7 and 8, have been computed with four basis sets and their results are shown in Table 5, whilst the most reliable structures, calculated at the B3LYP/AUG-cc-pVDZ level, are depicted in Fig. 8. A number of conclusions can be advanced from Table 5 and the comparison with the experimental binding energies (Table 2). First, the values calculated at B3LYP/6-31G are too high, even after applying the BSSE correction (one should note that the counterpoise procedure yields

Table 3
Structural parameters for the MPEA conformers, calculated at B3LYP/6-311+g* level distances in Å, angles in degrees and energies in $cm^{-1}$

| | Conformer | | | | | | | | |
|---|---|---|---|---|---|---|---|---|---|
| | 1 | 2 | 3 | 4 | 5 | 6 | 7 | 8 | 9 |
| Peak Assignment | E | F | G | D | B | – | C | A | – |
| $NH_a$ | 1.015 | 1.016 | 1.016 | 1.016 | 1.016 | | 1.016 | 1.016 | |
| $NH_b$ | 1.015 | 1.015 | 1.015 | 1.015 | 1.015 | | 1.015 | 1.015 | |
| $C_\alpha N$ | 1.462 | 1.467 | 1.467 | 1.4621 | 1.466 | | 1.461 | 1.466 | |
| $C_{Ring}\cdots HN$ | – | – | – | 3.000 | 2.875 | | 3.011 | 2.907 | |
| $\omega^a$ | −90.2 | −92.7 | −92.5 | −81.6 | −83.5 | | −97.9 | −97.8 | |
| $C_1C_\alpha C_\beta N$ | 179.9 | 178.5 | −177.8 | −62.1 | −64.2 | | 62.4 | 64.3 | |
| *Relative* $E^0$ | | | | | | | | | |
| B3LYP/6-31+G* | 7 | 70 | 86 | 61 | 34 | 551 | 49 | 0 | 520 |
| B3LYP/6-311+G* | 18 | 68 | 87 | 73 | 34 | – | 59 | 0 | – |
| B3LYP/AUG-cc-pVDZ | 11 | 28 | 38 | 88 | 31 | – | 67 | 0 | – |

[a] Angle between the aromatic ring and the $C_\alpha$–$C_\beta$ bond.

an estimation of the BSSE, not the accurate value). Second, the computed binding energies with basis set including diffuse and polarisation functions (e.g. in a 6-31+g* basis set), are in good agreement with the experimental values (Table 2) and the BSSE decreases to ~1/3 of the value computed by the 6-31g basis set. Third, the enlargement from double-ζ to triple-ζ basis sets, with some ~20% increase in the number of basis functions, is not mirrored in the calculated binding energies. On the contrary, both binding energies and the BSSE corrections are higher. Fourth, Dunnig's double-ζ basis set, including polarisation and diffuse functions both in heavy and hydrogen atoms – to a total of 411 basis functions for the complex – yields binding energies in very good agreement with the experiments and BSSE corrections half than those calculated using the 6-31+g* basis set. Furthermore, the isomer stability sequence has the same pattern as the lower level basis sets studied. In consequence, the addition of diffuse and polarisation functions on the hydrogen atoms improves the description of the system rather more than including extra p orbitals on the heavy atoms. In addition, data in Table 5 indicate that the good agreement between experimental and calculated values at B3LYP/6-31+G* level is somewhat accidental, as an increase in the basis sets does not predictably improve the computed energies.

Taking note of the small BSSE energy correction of the B3LYP/AUG-cc-pVDZ calculation, one may assign the two most stable structures, and therefore the two observed isomers, to the CF8I3 and CF5I3 conformers. These structures have been used as precursors in the optimisation of the cation species, yielding the following binding energies: $D_0(I_0) = 1981$ $cm^{-1}$ for the CF8I3 cation (hereafter referred to as CF8I3-C) and 1759 $cm^{-1}$ for the CF5I3 cation (hereafter CF5I3-C). The computed IE for the CF8I3-C and CF5I3-C cations are 60,421 and 60,453 $cm^{-1}$ respectively. It is worth pointing out that optimisation of the CF7I3-C and CF4I3-C structures was also attempted without success, as the bare molecule always evolves to the CF6 and CF9 structures, with the N atom lone pair interacting with the aromatic ring, and the water molecule shifting towards an $N–H\cdots OH_2$ proton acceptor position.

## 5. Discussion

### 5.1. Structure assignment

Among the fundamental properties providing hints to assign the isomers spectral bands to the computed structures the following are considered here: the ground state binding energies, the ground state vibrational modes, the binding energies of the cation and the IE. As discussed above, the computed CF8I3 structure is the most stable and is expected to be associated with the most intense

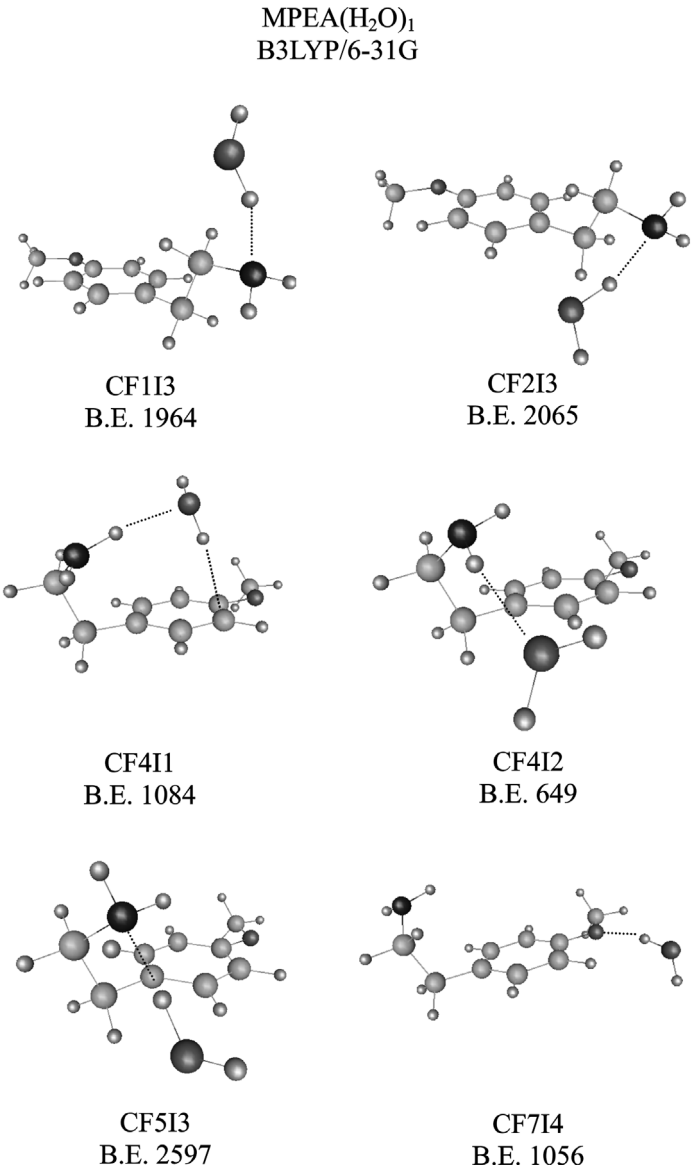


Fig. 7. Some computed stable geometries of the MPEA$(H_2O)_1$ isomers calculated at the B3LYP/6-31G level and labelled as CF*n*I*m* ($m = 1$–4; with $m = 1$ for the solvent water bonded to the N–$H_a$, $m = 2$ to the N–$H_b$, $m = 3$ to the N atom and $m = 4$ to the O–$CH_3$ group).

band of the spectrum, i.e. to isomer II; and, by exclusion, the CF5I3 to isomer I. According to the experimental data depicted in Table 2, isomers I and II yield ground binding energies of 1865 and 1730 $cm^{-1}$ respectively, while the computed dissociation energies of the CF5I3 and CF8I3 structures are 1681 and 1784 $cm^{-1}$ (Table 5). Therefore, the experimental and computed relative stability trend of the isomers is opposite. If one arbitrarily exchanges the assignment and identifies isomer I to the CF8I3 structure and isomer II to CF5I3, the ground dissociation energies turn out to be: $D_0(S_0) = 1579$ $cm^{-1}$ for isomer I and 2016 $cm^{-1}$ for isomer II, values too large to justify the

Table 4
BSSE and ZPE corrected binding energies and estimated BSSE (in parentheses) for the 36 MPEA$(H_2O)_1$ calculated isomers at the B3LYP/6-31G level[a]

| Conformer | Isomers | | | |
|---|---|---|---|---|
| | 1 | 2 | 3 | 4 |
| 1 | CF1I1<br>641<br>(781) | CF1I2<br>659<br>(736) | CF1I3<br>1964<br>(889) | CF1I4<br>1085<br>(1284) |
| 2 | CF2I1<br>goes to<br>CF2I3 | CF2I2<br>goes to<br>CF2I3 | CF2I3<br>2065<br>(1358) | CF2I4<br>1091<br>(1286) |
| 3 | CF3I1<br>goes to<br>CF3I3 | CF3I2<br>goes to<br>CF3I3 | CF3I3<br>2135<br>(1184) | CF3I4<br>1080<br>(1283) |
| 4 | CF4I1<br>1084<br>(1078) | CF4I2<br>649<br>(826) | CF4I3<br>2150<br>(827) | CF4I4<br>1068<br>(1284) |
| 5 | CF4I1<br>975<br>(1141) | CF5I2<br>goes to<br>CF5I3 | CF5I3<br>3056<br>(1370) | CF5I4<br>1072<br>(1282) |
| 6 | CF6I1<br>goes to<br>CF5I1 | CF6I2<br>goes to<br>CF5I3 | CF6I3<br>goes to<br>CF5I3 | CF6I4<br>1154<br>(1285) |
| 7 | CF7I1<br>972<br>(1237) | CF7I2<br>goes to<br>CF5I3 | CF7I3<br>2168<br>(819) | CF7I4<br>1056<br>(1281) |
| 8 | CF8I1<br>863<br>(1367) | CF8I2<br>goes to<br>CF8I3 | CF8I3<br>2950<br>(1449) | CF8I4<br>1079<br>(1283) |
| 9 | CF9I1<br>goes to<br>CF8I1 | CF9I2<br>goes to<br>CF8I3 | CF9I3<br>goes to<br>CF8I3 | CF9I4<br>1138<br>(1291) |

[a] The nomenclature to label the complex is also included in the upper row of data for each conformer. CF*n* stands for the bare molecule conformation in the complex and I*m* refers to the position of the water molecule in the complex: $m = 1$ attached to N–$H_a$, $m = 2$ attached to N–$H_b$, $m = 3$ attached to the N atom and $m = 4$ bonded to the oxygen atom lone pair. In Fig. 7 some examples are offered.

Table 5
BSSE and ZPE corrected binding energies and estimated BSSE for the seven most stable MPEA$(H_2O)_1$ isomers, as calculated at four levels: B3LYP/6-31G, B3LYP/6-31+G*, B3LYP/6-311+G* and B3LYP/AUG-cc-pVDZ (Experimental binding energies are shown in Table 2)

| | Basis set | | | |
|---|---|---|---|---|
| | 6-31g | 6-31+g* | 6-311+g* | AUG-cc-pVDZ |
| No. of basis functions | 138 | 258 | 309 | 411 |
| *CF1I3* | | | | |
| $E^0$ | 1964 | 1743 | 1749 | 1479 |
| BSSE | *889* | *387* | *415* | 178 |
| $E^0_{relative}$ | 1094 | 214 | 390 | 305 |
| *CF2I3* | | | | |
| $E^0$ | 2065 | 1776 | 1867 | 1559 |
| BSSE | *1358* | *419* | *419* | 215 |
| $E^0_{relative}$ | 991 | 254 | 281 | 225 |
| *CF3I3* | | | | |
| $E^0$ | 2135 | 1738 | 1863 | 1482 |
| BSSE | *1184* | *421* | *418* | *252* |
| $E^0_{relative}$ | 92 | 299 | 304 | *302* |
| *CF4I3* | | | | |
| $E^0$ | 2150 | 1856 | 1948 | 1637 |
| BSSE | *827* | *386* | *373* | *172* |
| $E^0_{relative}$ | 906 | 156 | 205 | 147 |
| *CF513* | | | | |
| $E^0$ | 3056 | 1877 | 1920 | 1681 |
| BSSE | *1370* | *470* | *533* | *244* |
| $E^0_{relative}$ | 0 | 108 | 194 | *103* |
| *CF713* | | | | |
| $E^0$ | 2168 | 1803 | 2139 | 1601 |
| BSSE | *819* | *397* | *403* | *189* |
| $E^0_{relative}$ | 888 | 197 | 0 | 183 |
| *CF813* | | | | |
| $E^0$ | 2950 | 1951 | 2012 | 1784 |
| BSSE | *1449* | *460* | *528* | *189* |
| $E^0_{relative}$ | 106 | 0 | 68 | 0 |

observed relative intensities of the origin bands (Table 2). In consequence, the original assignment of isomer II to the CF8I3 structure still seems to be the most likely.

Although the computed vibrational normal modes of both isomers are similar and only a few lines are actually observed in the spectrum (Table 6), isomer I vibrational modes are slightly red-shifted with respect to those of isomer II. The same pattern is found for the CF5I3 structure with respect to that of CF8I3. Therefore, the comparison of vibrational modes leads to identify isomer I to the CF5I3 structure and isomer II to CF8I3.

Before comparing the calculated and the experimental dissociation energies, $D_0(I_0)$, it is worth remembering that experimental $D_0(I_0)$ is computed as the difference between the $I_0 \leftarrow S_1$ and the

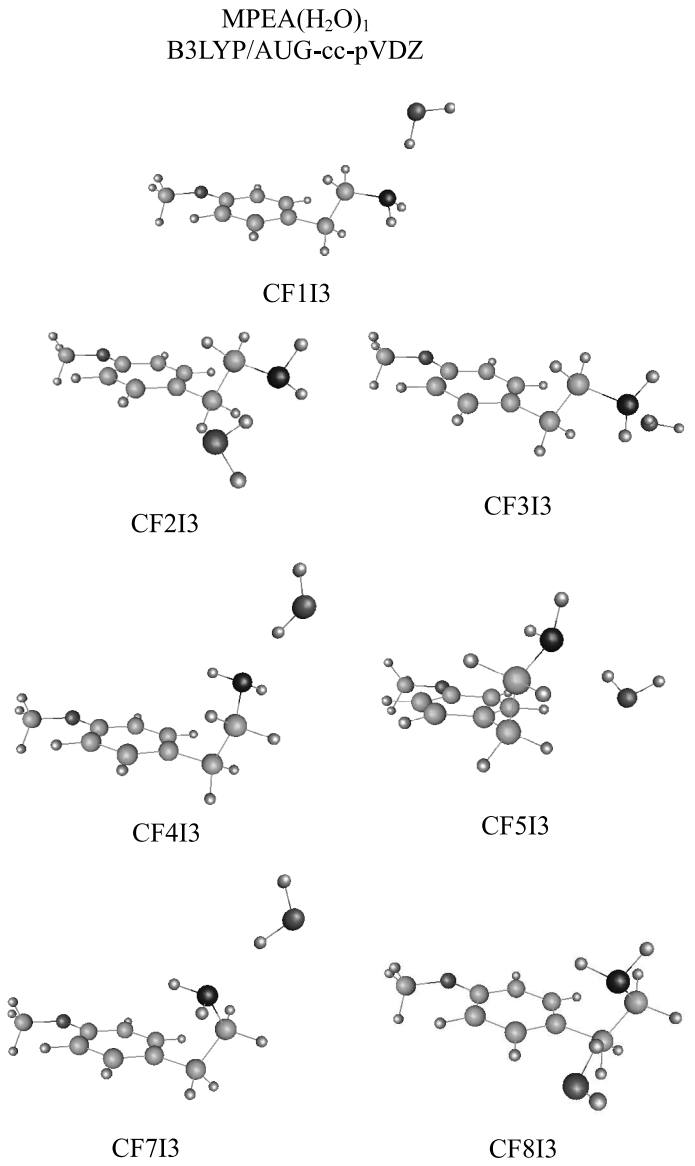


Fig. 8. Computed stable geometries of the MPEA$(H_2O)_1$ isomers calculated at the B3LYP/AUG-cc-pVDZ level and labelled as CF$n$I3 ($n = 1$–5, 7 and 8, depending on the bare conformer).

fragmentation $\leftarrow S_1$ transition energies and thus is independent of the precursor conformer of the complex. The experimental $D_0(I_0)$ of the isomers are 2279 $cm^{-1}$ for isomer I and 2459 $cm^{-1}$ for isomer II, which compares with that calculated of 1759 $cm^{-1}$ (CF5I3-C) and 1981 $cm^{-1}$ (CF8I3-C). In consequence, the favoured assignment is isomer I to the CF5I3-C structure (and isomer II to CF8I3-C), despite the fact that the disagreement between experimental and calculated energies is larger than for the ground dissociation energy, $D_0(S_0)$.

Isomer IEs computed as the difference of the cation and the ground absolute energies yield

Table 6
Intermolecular normal modes of the CF5I3 and the CF8I3 complexes as calculated at the B3LYP/AUG-cc-pVDZ level, and comparison with the experimental values

| Mode | Description | CF5I3 | | CF8I3 | |
|---|---|---|---|---|---|
| | | $cm^{-1}$ | Experimental value[a] | $cm^{-1}$ | Experimental value[b] |
| 1 | $\beta + \tau$ | 26 | 28 | 34 | 32 |
| 3 | $\tau + \tau(C_1–C_\beta)$ | 60 | 64 | 64 | |
| 5 | $\rho_w$ | 86 | | 98 | |
| 8 | $\sigma$ | 184 | | 185 | |
| 9 | $\sigma$ + b.m.[c] | 213 | | 210 | |
| 18 | $\rho_r + \tau(C_\alpha–N)$ | 510 | | 517 | |

[a] A mode at 37 $cm^{-1}$ is assigned as $\nu_2 = \tau(C_1–C_\beta) = 43$ $cm^{-1}$, and the mode at 75 $cm^{-1}$ as $2\nu_2$. A third mode at 791 $cm^{-1}$ is assigned as $\nu_{19} = 17b = 823$ $cm^{-1}$.
[b] A mode at 38 $cm^{-1}$ is assigned as $\nu_2 = \tau(C_1–C_\beta) = 45$ $cm^{-1}$, and the mode at 74 $cm^{-1}$ as $2\nu_2$. A third mode at 815 $cm^{-1}$ is assigned as $\nu_{19} = 17b = 823$ $cm^{-1}$.
[c] Intermolecular mode coupled with a bare molecule complicated mode.

60,421 $cm^{-1}$ for CF8I3 and 60,453 $cm^{-1}$ for CF5I3, and compares with the experimental IE of 63,298 $cm^{-1}$ for isomer I and 63,269 $cm^{-1}$ for isomer II. Although the theoretical IEs are consistently smaller than the experimental ones by ≈3000 $cm^{-1}$, their relative differences are very close (32 $cm^{-1}$ compared to 29 $cm^{-1}$). Although the energy shift pattern points to the existence of a source of systematic error in the calculation of both isomers, the comparison of calculated and experimental energies is taken as a useful guide for isomer assignment. Accordingly isomer I is again identified to the CF5I3 geometry (and isomer II to CF8I3).

In summary, all the assignment methods employed but one, the $D_0(S_0)$ relative energies, plausibly associate isomers I and II to the CF5I3 and CF8I3 structures. It is worth noting that the experimental and calculated $D_0(S_0)$ energies for CF8I3 differ by only 3%, while for CF5I3 it is ~10%, differences that cannot be regarded as large either. The main source of inaccuracies in the experimental determination of $D_0(S_0)$ energies stems from the low signal-to-noise ratio of the fragmentation $\leftarrow S_1$ transition energy. Three extrapolation measurements of the FE profiles were carried out, yielding 30,028, 30,069 and 30,022 $cm^{-1}$ (mean value 30,039 $cm^{-1}$) for isomer II and 29,926, 29,943 and 29,836 $cm^{-1}$ (mean value 29,901 $cm^{-1}$) for isomer I. As can be readily appreciated, the FE accuracy for isomer II, with good signal-to-noise ratio, is better than for isomer I. Furthermore, the isomers binding energies difference are within the experimental error, and it is concluded that the experimental and theoretical isomers stability disagreement is due to experimental inaccuracies of the CF5I3 $D_0(S_0)$ energy.

### 5.2. Isomer structures and stability

Although the strongest intermolecular interaction within the $MPEA(H_2O)_1$ complex is the H-bond, there are some weaker interactions that shapes the complex and add some extra stability. Thus, in CF*n*I3 isomers, there exists an interaction between the water oxygen and the nearest hydrogen atoms (see Table 7). The orientations of the ethylamino group lead to "secondary" interactions of the water molecule with the solvation site, changing its neighbourhood even in the *anti* conformers. For example, the water oxygen atom interacts with the $C_\beta$ hydrogen atom at a distance of 2.857 Å for the CF2I3 structure and 2.669 Å for the CF3I3. The interaction takes place at a van der Waals (vdW) interaction distance and thus, it is much weaker than the H-bond. In addition, the isomers have an even weaker interaction between the water oxygen and the $C_\alpha$ hydrogen atom, at a distance of ~3.2 Å.

In the CF5I3 and CF8I3 folded conformers, the position of the water molecule enables an inter-

Table 7
Selected structural parameters of the most stable $MPEA(H_2O)_1$ complexes, formed from the bare molecule conformers. CF6 and CF9 conformers have not been included because they evolve into other conformers

| | CF*n*I3 | | | | | | |
|---|---|---|---|---|---|---|---|
| | $n=1$ | $n=2$ | $n=3$ | $n=4$ | $n=5$ | $n=7$ | $n=8$ |
| $N–H_a$ | 1.019 | 1.018 | 1.018 | 1.018 | 1.019 | 1.019 | 1.019 |
| $N–H_b$ | 1.019 | 1.019 | 1.019 | 1.019 | 1.017 | 1.019 | 1.017 |
| $C_\alpha–N$ | 1.472 | 1.477 | 1.478 | 1.471 | 1.476 | 1.471 | 1.476 |
| $C_{ring}\cdots HN$ | – | – | – | – | 2.851 | 3.034 | 2.867 |
| $\omega$[a] | 90.1 | 91.7 | 93.1 | 99.5 | 82.8 | 102.4 | 96.9 |
| $C_1C_\beta C_\alpha N$[b] | 179.7 | 175.3 | 174.9 | 61.9 | 62.0 | 62.2 | 62.5 |
| $OH_a$ | 0.982 | 0.983 | 0.984 | 0.983 | 0.985 | 0.983 | 0.985 |
| $OH_b$ | 0.963 | 0.963 | 0.963 | 0.963 | 0.963 | 0.963 | 0.963 |
| HOH | 105.4 | 105.6 | 105.8 | 105.4 | 105.8 | 105.4 | 105.8 |
| $HO–H\cdots NH_2$ | 1.922 | 1.919 | 1.919 | 1.913 | 1.909 | 1.913 | 1.911 |
| $HC_\alpha–H\cdots OH_2$ | 3.417 | 3.177 | 3.267 | 2.778 | – | 2.757 | – |
| $HC_\beta–H\cdots OH_2$ | – | 2.857 | 2.669 | – | 2.739 | – | 2.827 |
| $C_{ring}\cdots OH_2$ | – | – | – | – | 2.701 | – | 2.648 |

[a] Angle between the ring aromatic plane and the $C_\beta C_\alpha$ bond.
[b] Dihedral angle.

action of its oxygen atom with one of the hydrogen atoms bonded to the aromatic ring, at computed distances of 2.701 and 2.648 Å respectively. The isomer with the shortest interaction distance to the ring also has the largest spectral shift. In a previous study on the ethyl-*p*-aminobenzoate/water complexes ($EAB(H_2O)_1$), the same behaviour was also observed [22]. However, it is doubtful that the observed shift can be associated to the interaction of the hydrogen atoms of the aromatic ring or to the change of the strength in the H-bond. Upon complex electronic excitation, the charge density of the aromatic ring spreads, and the strength of the $N–H\cdots\pi$ interaction decreases, weakening the $HO–H\cdots NH_2$ interaction, and resulting in a blue-shift. As the CF8I3 structure has the strongest H-bond, it is not surprising that it also presents the largest shift.

In addition to the solvent interaction with the hydrogen atoms attached to the benzene ring, all the folded conformers have interactions with the aliphatic hydrogen atoms at distances of ~2.7–2.8 Å, again a much weaker interaction than the H-bond but sizeable enough to influence the geometry of the complex. These secondary interactions make the optimisation of the complex structure a hard task.

In the correlation of the chromophore and the 1:1 water complex structures, the contrast between the seven conformers of the precursor and the two isomers of the complex is remarkable. There are three possible arguments to explain the absence of some isomers: the changes in binding energies, the absence of isomerisation barriers and the unfavourable Frank–Condon factors for either excitation or ionisation. Inspection of Table 5 shows the presence of sensible energy differences between the *anti* and *gauche* species, though too small between the *gauche* isomers to justify the absence of the CF4I3 and CF7I3 species. In addition, the attachment of one water molecule would release an energy equal to the complex binding energy in the molecular vibrational modes. This energy is used by the solvent to move between solvation sites or by the bare molecule to change between conformers to finally arrive at the most stable structure.

Finally, the attempts to optimise the CF4I3 and CF7I3 ion structures were fruitless, evolving to geometries with the $NH_2$ lone pair near the aromatic $\pi$-electron and the water molecule accepting one $NH_2$ proton. If such a structure were correct, the Frank–Condon factors of the $I_0 \leftarrow S_1$ transition would be so adverse that the CF4I3 and CF7I3 structures would never be observed by REMPI and R2PI spectroscopies, whilst they would be observed in a simple LIF experiment. However, the hidden isomers and the bare

molecule spectral bands overlap which precludes their study.

### 5.3. Calculations with various basis sets

The corrected binding energies of $MPEA(H_2O)_1$ depicted in Table 5 illustrates that DFT calculations conducted with small size basis sets yield sensible estimations of complex properties. Table 8 shows a comparison between the main structural parameters of the H-bond site and its neighbourhood for the most stable isomer, CF8I3, calculated with the 6-31g, 6-31+g*, 6-311+g* and AUG-cc-pVDZ basis sets. It is obvious that calculations with the simplest basis set satisfactorily describe most bare molecule parameters, although the shortest distance among the aromatic ring carbon and the H atom of the $NH_2$ group, $C_{ring}\cdots HN$, is poorly described. However, a good description of the H-bond properties requires diffuse and polarisation functions on the heavy atoms. The most elusive parameters to describe are those related to the position of the water molecule: the dihedral angle with respect to the $NH_2$ moiety and the distances to the bare molecule H atoms subject to interaction. An inspection of Table 8 shows that the B3LYP/6-31+G* level offers an accurate enough description of all these parameters, in some cases superior to the B3LYP/6-311+G* level (cf. the distance between the water oxygen atom and the closest aromatic hydrogen atoms, $C_{ring}$–$H\cdots OH_2$). The pattern of relative interactions yielded at the B3LYP/6-31+G* level is significant: $O$–$H_a\cdots NH_2$ distance $<$ $C_{ring}$–$H\cdots OH_2$ $<$ $C_\beta$–$H\cdots OH_2$, identical to that found at the B3LYP/AUG-cc-pVDZ extended basis set level.

Table 8
Comparison of the structural parameters of the most stable $MPEA(H_2O)_1$ complexes, obtained at different calculation levels

| | B3LYP | | | |
|---|---|---|---|---|
| | 6-31G | 6-31+G* | 6-311+G* | AUG-cc-pVDZ |
| N–$H_a$ | 1.019 | 1.021 | 1.017 | 1.019 |
| N–$H_b$ | 1.017 | 1.019 | 1.016 | 1.017 |
| $C_\alpha$–N | 1.484 | 1.477 | 1.467 | 1.476 |
| $C_{ring}\cdots HN$ | 2.783 | 2.889 | 2.892 | 2.867 |
| $\omega$[a] | 94.5 | 97.6 | 97.9 | 96.9 |
| $C_1C_\beta C_\alpha N$[b] | 60.1 | 61.6 | 61.5 | 62.5 |
| $OH_a$ | 1.007 | 0.990 | 0.984 | 0.985 |
| $OH_b$ | 0.974 | 0.968 | 0.962 | 0.963 |
| HOH | 110.9 | 106.6 | 108.2 | 105.8 |
| $HO$–$H\cdots NH_2$ | 1.772 | 1.896 | 1.897 | 1.991 |
| $HC_\beta$–$H\cdots OH_2$ | 2.432 | 2.782 | 2.711 | 2.827 |
| $C_{ring}\cdots OH_2$ | 2.392 | 2.568 | 2.488 | 2.648 |
| Angle $OH_aN$ | 110.9 | 106.6 | 108.2 | 105.8 |
| $H_aOH_bN$[b] | 160.6 | 176.0 | 171.8 | 177.4 |

[a] Angle between the ring aromatic plane and the $C_\beta C_\alpha$ bond.
[b] Dihedral angles.

### 5.4. Vibrational assignment

Due to the molecular asymmetry induced by the methoxy group on the aromatic π-system and to the multidimensional shape of the PES of the solute–solvent interaction, a simple description of the complex normal modes such as bending, stretching, etc., is neither easy nor sensible. So, the $\nu_1$ normal mode is better described as a jumping of the oxygen atom among the two close hydrogen atoms, the $C_{ring}$–H and the $C_\beta$–H. In addition, the strong coupling between the intra- and the intermolecular normal modes causes large shifts in some bare molecule vibrational modes. For example, the bare molecule $\nu_8$ band at 275 $cm^{-1}$ ($\tau(C_\alpha$–N)) blue-shifts to 303 $cm^{-1}$ in the CF8I3 isomer and then it includes a rocking motion of the water molecule. The most noticeable shift is the bare molecule $\nu_{22}$ band at 842 $cm^{-1}$ that red-shift to 737 $cm^{-1}$ in the CF8I3 complex. Although the number of experimental vibrations is small, the agreement with the calculated frequencies is excellent, allowing an unambiguous identification of all the observed modes.

## 6. Conclusions

The experimental and theoretical study of the $MPEA(H_2O)_1$ isomers reported uses a set of mass-resolved spectroscopies and DFT ab initio calculations at the B3LYP/6-31G, B3LYP/6-31+G*, B3LYP/6-311+G* and B3LYP/AUG-cc-pVDZ levels. HB spectroscopy has been used to conclusively show the existence of two $MPEA(H_2O)_1$ isomers, derived from a precursor with seven

known conformers. Binding energies were determined by the fragmentation threshold method and are $D_0(S_0) = 1730$ cm$^{-1}$, $D_0(S_1) = 1546$ cm$^{-1}$ and $D_0(I_0) = 2279$ cm$^{-1}$ for isomer I and $D_0(S_0) = 1865$ cm$^{-1}$, $D_0(S_1) = 1735$ cm$^{-1}$ and $D_0(I_0) = 2459$ cm$^{-1}$ for isomer II. The comparison of experimental results with ab initio calculations leads to the identification of both isomer structures and vibrational frequencies. Isomer I is consistent with the CF5I3 calculated structure, with a (BSSE and ZPE corrected) binding energy of 1681 cm$^{-1}$, and isomer II to the most stable CF8I3 structure, with a binding energy of 1784 cm$^{-1}$. Although the strongest interaction of the isomers is the HO–H$\cdots$NH$_2$ hydrogen bond there are interactions with the aliphatic and the aromatic hydrogen atoms that shapes the final structures.

The DFT calculations were conducted for four basis sets and show that small basis set (B3LYP/6-31+G* level) yields good estimates of the binding energies and the structures. It is also concluded that p orbitals added to the heavy atoms do not improve the binding energies, whilst p orbitals and diffuse functions on the hydrogen atoms (with the B3LYP/AUG-cc-pVDZ level) significantly improve the binding energy.

## Acknowledgements

We acknowledge the grants and complimentary support from DGES (PB91-0510, PB95-0510 and PB96-1472), the Basque Government and the UPV. JAF thanks DGES for the award of a personal contract and I.U. and A.L. thank the Basque Government for their post-graduate fellowship.

## References

[1] S.J. Martinez III, J.C. Alfano, D.H. Levy, J. Mol. Spectrosc. 158 (1993) 82.
[2] J. Yao, H.S. Im, M. Foltin, E.R. Bernstein, J. Phys. Chem. A. 104 (2000) 6197.
[3] P.D. Godfrey, L.D. Hatherley, R.D. Brown, J. Am. Chem. Soc. 117 (1995) 8204.
[4] S. Sun, E.R. Bernstein, J. Am. Chem. Soc. 120 (1998) 2622.
[5] J.A. Dickinson, M.R. Hockridge, R.T. Kroemer, E.G. Robertson, J.P. Simons, J. McCombie, M. Walker, J. Am. Chem. Soc. 120 (1998) 2622.
[6] J.J. Urban, C.W. Cronin, R.R. Roberts, G.R. Famini, J. Am. Chem. Soc. 119 (1997) 12292.
[7] I. Unamuno, J.A. Fernández, A. Longarte, F. Castaño, J. Phys. Chem. A 104 (2000) 4364.
[8] M. Satta, A. Latini, S. Piccirillo, T.M. Di Palma, M. Scuderi, M. Sperenza, A. Giardini, Chem. Phys. Lett. 316 (2000) 94.
[9] S.R. Haines, C.E.H. Dessent, K.J. Müller-Dethlefs, J. Chem. Phys. 111 (1999) 1947.
[10] A. Longarte, J.A. Fernández, I. Unamuno, F. Castaño, J. Chem. Phys. 112 (2000) 3170.
[11] M.J. Frisch, G.W. Trucks, H.B. Schlegel, G.E. Scuseria, M.A. Robb, J.R. Cheeseman, V.G. Zakrzewski, J.A. Montgomery Jr., R.E. Stratmann, J.C. Burant, S. Dapprich, J.M. Millam, A.D. Daniels, K.N. Kudin, M.C. Strain, O. Farkas, J. Tomasi, V. Barone, M. Cossi, R. Cammi, B. Mennucci, C. Pomelli, C. Adamo, S. Clifford, J. Ochterski, G.A. Petersson, P.Y. Ayala, Q. Cui, K. Morokuma, D.K. Malick, A.D. Rabuck, K. Raghavachari, J.B. Foresman, J. Cioslowski, J.V. Ortiz, B.B. Stefanov, G. Liu, A. Liashenko, P. Piskorz, I. Komaromi, R. Gomperts, R.L. Martin, D.J. Fox, T. Keith, M.A. Al-Laham, C.Y. Peng, A. Nanayakkara, C. Gonzalez, M. Challacombe, P.M.W. Gill, B. Johnson, W. Chen, M.W. Wong, J.L. Andres, C. Gonzalez, M. Head-Gordon, E.S. Replogle, J.A. Pople, GAUSSIAN98, Revision A.7, Gaussian, Inc., Pittsburgh PA, 1998.
[12] A. Berces, T. Ziegler, J. Chem. Phys. 98 (1993) 4793.
[13] B.G. Johnson, P.M. Gill, J.A. Pople, J. Chem. Phys. 98 (1993) 5612.
[14] N.C. Handy, C.N. Murray, R.D. Amos, J. Phys. Chem. 97 (1993) 4392.
[15] G. Rauhut, P. Pulay, J. Phys. Chem. 99 (1995) 3093.
[16] R.G. Parr, W. Yang, Density Functional Theory of Atoms and Molecules, Oxford University Press, New York, 1989.
[17] A. Longarte, J.A. Fernández, I. Unamuno, F. Castaño, Chem. Phys. Lett. 308 (1999) 516.
[18] J.A. Fernández, A. Longarte, I. Unamuno, F. Castaño, J. Chem. Phys. 113 (2000) 5804.
[19] J.A. Fernández, A. Longarte, I. Unamuno, F. Castaño, J. Chem. Phys. 113 (2000) 8541.
[20] A. Longarte, J.A. Fernández, I. Unamuno, F. Castaño, J. Chem. Phys. 113 (2000) 8549.
[21] A. Longarte, J.A. Fernández, I. Unamuno, F. Castaño, Chem. Phys. 260 (2000) 83.
[22] J.A. Fernández, A. Longarte, I. Unamuno, F. Castaño, J. Chem. Phys. 113 (2000) 8531.